Title : Remote sensing classification of Japanese knotweed in the Netherlands riparian and urban areas.

05-07-2023
Mikolaj Soltysiuk 6860567

1 INTRODUCTION

Invasive alien plant species (IAPS) have become a significant concern due to their detrimental effects on ecosystems, biodiversity, and ecological processes (Langmaier & Lapin, 2020; Paz-Kagan et al., 2019; Guido et al., 2017). Among the various IAPS, Japanese knotweed (Fallopia japonica) stands out as one of the most problematic species globally (DAISIE, 2008; ISSG/IUCN, 2009). Originally from East Asia, Japanese knotweed was introduced to different regions for ornamental purposes, erosion control, and as a forage crop (Conolly, 1977).

Once it escapes from cultivation, Japanese knotweed establishes itself in diverse habitats, including coastal areas, riparian zones, urban environments, and wetlands (Conolly, 1977; Pyšek & Prach, 1993; Rouifed et al., 2011). Its rapid and aggressive growth, coupled with its ability to outcompete native species, leads to negative impacts on soil characteristics, ecosystem functioning, and infrastructure (Aguilera et al., 2010; Collingham

et al., 2000; DAISIE, 2008; Smith et al., 2007). The resilient rhizome system of Japanese knotweed and its resistance to eradication efforts make its control challenging (Shaw & Seiger, 2002).

Standing biomass may collect and provide a fire risk as a result of the slow rate of decomposition of leaves and stalks (Seiger & Merchant, 1997). In central Europe, the spread of F. japonica is primarily vegetative. It occurs due to people's movement of contaminated soil or the dispersal of rhizomes or cane pieces via waterways, highways, and railroads (Conolly, 1977; Pyek et al., 2003; Smith et al., 2007). Aside from being encouraged by increased CO2 and N deposition rates, the spread of F. japonica is progressively accelerating across Europe (Bradford et al., 2007, DAISIE, 2008). Once established, F. japonica is exceptionally challenging to get rid of. The process may require multiple treatments, and removal efforts may have a negative effect on the soil or plants(Shaw& Seiger,2002).

Control techniques created for the avoidance of new invaders, detecting early-stage invasions, rapid response, and managing established or spreading IAPS can mitigate these effects (IUCN 2000). Early detection can help save money on the significant financial resources needed to eradicate, contain, and control established IAPS. The technique requires the most precise data on the spatial distribution and degrees of IAPS infestation to succeed.

Datasets of the IAPS's geographic distribution were previously primarily gathered through field surveys, in-situ inventories gathered by GNSS (Global Navigation Satellite Systems), or through the analysis of aerial photographs (Jombo et al., 2021; Royimani et al., 2019; Hartling et al., 2019; Lawrence et al., 2006; Müllerová et al., 2005). However, these techniques require much labor and are frequently unsuitable from a technical and cost standpoint, mainly when dealing with significant or inaccessible areas. Their dependence on the observer may also be somewhat subjective (Royimani et al., 2019; Lawrence et al., 2006). Despite limitations linked to the availability and resolution of pictures (Robinson et al., 2016), remote sensing may be a more advantageous alternative for monitoring and managing IAPS (Dash et al., 2019; Niphadkar & Nagendra, 2016). Current research proves that Japanese knotweed classification results vary(Hick, 2021 & Martin et al.,2018) Few of the main crucial components to success that we emphasize and compare between previous studies are: Data type, Method, spatial resolution, and Number of bands.

Our study uses two different RS imagery sets/Data types: aerial and satellite images. Aerial images have a much higher spatial resolution concerning satellite data And have been successfully proven to detect Japanese knotweed (Dorigo et al., 2012). The author's research classified Japanese knotweed with 98.1% accuracy. They used NIR, Bi-temporal band ratio, and NDVI to detect Japanese knotweed in Slovenia. Satellite data, however, can have a higher spectral band distinction. Another highly successful example of detecting Japanese knotweed is the (Hick,2021) study. In this paper, the author used multidimensional data to detect Invasive alien species in Cardiff. Through the analysis of hyperspectral VHR data containing 186 bands, the author managed to get very high results across all alien invasive species and distinguish that Japanese knotweed is very separable around the VNIR region. In addition, CHM was derived from photogrammetry, and a threshold of 5m was applied to JK species. Another new example of satellite data being highly effective in detecting JK is a study conducted by (Nininahazawe et al., 2023), Where they used Worldview-3 and SPOT-7 satellites in the urban agglomeration of the Quebec City area. These two VHR data sources have 8 and 4 spectral bands. The authors performed mono-date and multi-date classification on this species, namely Japanese knotweed (Fallopia japonica), giant hogweed (Heracleum mantegazzianum), and phragmites (Phragmites australis). Using SVM, RF, and XGBoost, they confirmed the potential of remote sensing in the accurate mapping of Japanese knotweed, reaching the highest user accuracy of 90% using Worldview-3.

In order to get over the primary limitations of field inventory-based methodologies, automatic categorization techniques have been developed recently (Royimani et al., 2019; Lu & Weng, 2007; Lass et al., 2005). Mainly, nonparametric methods (such as machine learning techniques) and object-based image analysis (OBIA) have been employed extensively (Royimani et al., 2019; Asner et al., 2008; Lass et al., 2005). The OBIA that (Hick, 2021) used with Spatial angle mapper SAM was also performed by (Jones et al., 2011), where they used VHSR aerial imagery and NDVI to detect Japanese knotweed in Wales.

Nonparametric machine learning approaches can mix numerous data sources, frequently defined by different statistical distributions, because they do not require a normal distribution of training samples (Benediktsson & Sveinsson, 1997). In heterogeneous settings (such as urban regions), where it may be challenging to locate enough samples for particular classes, these approaches are also appropriate for small

samples (Masse, 2013). Until now most widely used algorithm for Japanese knotweed classification is RF, together with SVM, SAM, and XGBoost. A random forest approach was undertaken in IAS classification by (Martin et al., 2018). Two different locations in Spain were examined using Pleiades satellite and UAV imagery. The CHM and BTBRS proved that knotweed could be satisfactorily mapped, reaching 33% accuracy for Pleiades and 48% accuracy for UAVs. However, choosing the most appropriate method will depend on the scenery. In order to determine whether heterogeneity across many dates of photos could result in disproportionately harsh accuracy assessment and, consequently, poorly advised conclusions, they additionally rationalized errors of omission by imposing simple "buffer" borders around knotweed forecasts. One more case of detecting Japanese knotweed using a Random forest classifier in riparian areas was done by(Michez et al., 2016). They used UAS imagery in Wallonia to identify three different invasive alien species. However, this study concluded that more than the results are needed for operational work. Table 1 below reviews existing studies based on their study areas, data type, method, spatial resolution, number of bands and classification accuracy.

Author	Study Site	Data type	Method	Spatial resolution	Number of Bands	Classification Accuracy %
(Jones, Daniel, et al) 2011	Wales	Aerial imagery	OBIA, NDVI	40cm	4 bands (RGBIR)	(n.a)
(Dorigo, Wouter, et al.)2012	Ljubljana	Orthophotos	RF BTBR NDVI	50cm	4 bands (RGBNIR)	98.1%
(Michez, Adrien, et al .)2016	Wallonia	The Gatewing X100 UAS	RF	VHR(n.a.)	3 bands (RGB)	69%*
(François-Marie, et al)2018	Anse, Sierres	Pleiades, UAV	RF, CHM, MBTBRS, buffer	50cm, 8cm	4 Bands(RGBI)	33%, 48%
(Denise Hick)2021	Cardiff	HySpex VNIR + SWIR Phase One iXA 180	Hyperspectral, OBIA SAM NDVI CHM	VHR(n.a)	186	99.53%
(Nininahazwe, Fiston, et al.)2023	Quebec City	WorldView-3 SPOT-7	SVM, RF XGBoost	VHR(n.a.)	8 bands, 4 bands	88%

Table 1 Overview of existing research on the topic of Japanese knotweed clasification

Effective management depends on timely and accurate information about the geographic spread of Japanese knotweed. Invasive species like Japanese knotweed can be mapped and identified using remote sensing techniques (Dash et al., 2019; Niphadkar & Nagendra, 2016). Japanese knotweed has the potential to be reliably classified using machine learning techniques, notably object-based image analysis (OBIA), in conjunction with high-resolution multispectral imaging (Dorigo et al., 2012; Martin et al., 2018). PBIA, however, received less attention during remote sensing classification(Jimoh et al., 2021). This study aims to quantify the disparity in accuracy between these two image analysis techniques. Hyperspectral data performed the most influential research with this task, suggesting a improved with accuracy. The NDVI metric is applied in a few cases, with varying success of improvement (Dorigo et al., 2012 & Hick, 2021). There is also an inconsistent decision about machine learning algorithms that perform best for JK classification (Nininahazwe et al., 2023). The CHM was implemented to detect invasive alien species before, but not using LiDAR, just photogrammetry. Due to the time constraints of the study, the decision on data type was limited to free source. This resulted in obtaining Superview Neo and Pleiades imagery, along with Airborne and LiDAR data. This allows using of VHSR satellites while also comparing the User accuracy of Pleiades with previous research. Another potential gap in current research is the evaluation of mowed knotweed, which has not been conducted yet. To make these results transferable to future research, the study area is two different environments, riparian and urban. This paper aims to suggest and work with (the European Commission 2019) directive UE through invasive species mapping and improving the state of the art. This information can then be utilized to develop efficient strategies for controlling and eradicating this invasive species. This gives rise to a significant objective: Can remote sensing methods accurately monitor Japanese knotweed in urban and riparian areas?

Overall, this research seeks also to address the following minor objectives:

- Compare the performance of remote sensing methods, including pixel-based and object-based analyses, for monitoring Japanese knotweed.

- Analyze the results of the Support Vector Machines (SVM) and Random Trees (RT) models results on a given task.
- Investigate the potential benefits of incorporating the Canopy-Height Model and NDVI to improve classification accuracy.
- Assess the feasibility of identifying mowed Japanese knotweed using remote sensing techniques.

By achieving these objectives, we aim to contribute to the body of knowledge on remote sensing applications for Japanese knotweed monitoring, providing valuable insights for environmental agencies and waterboards involved in managing this invasive species.

The study used ArcGIS Pro to lay a framework that other WSP researchers or staff members can build upon and continue. Geographic information system (GIS) software, ArcGIS Pro, is widespread and offers solid spatial analysis, data management, and visualization tools. Its popularity and extensive acceptance in the workplace, which guarantees interoperability and facilitates communication with other WSP employees, led to its selection as the study's main piece of software. The software's comprehensive capabilities allowed for quick data processing, categorization, and spatial analysis, which made it possible to investigate and assess several remote sensing approaches for Japanese knotweed monitoring.

2 DATA COLLECTION AND STUDY SITES

As explained in Section 1, the main goal of this study is to classify Japanese knotweed into two distinct areas. Niuewegein represents the urban area, and the mouth of the river Geul represents the riparian area.

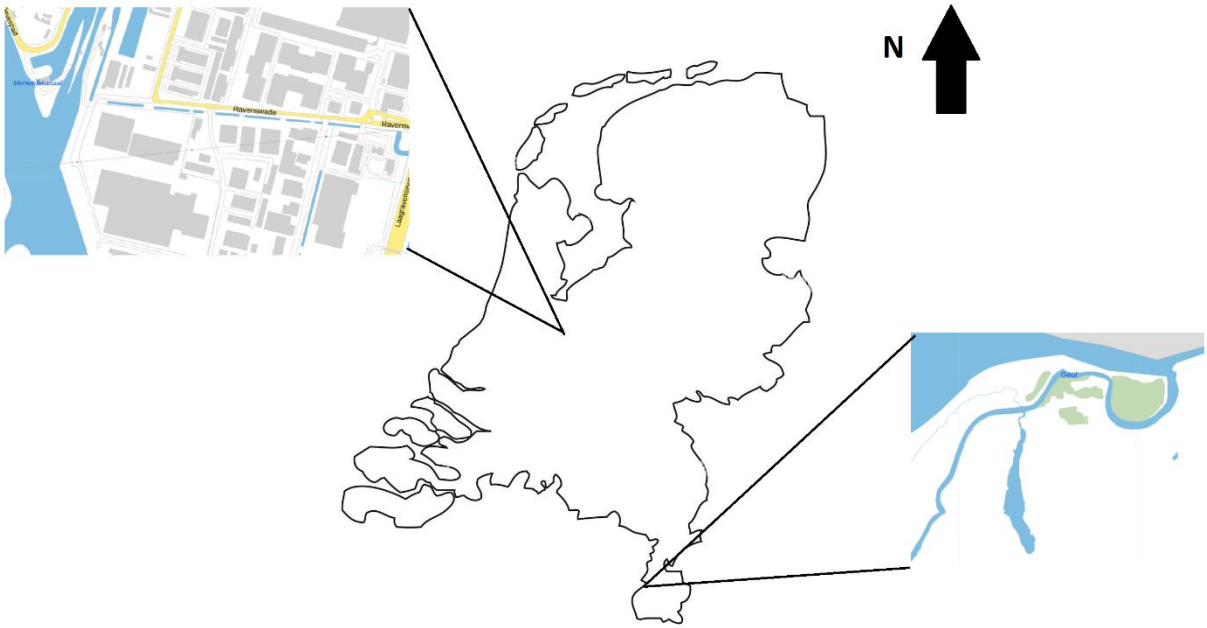

Different open-source data were extracted for each of these regions, namely satellite data, airborne photographs, and LiDAR scans. These were the best free, readily available maps of the ROI at this moment. High-resolution optical data for the research regions were gathered from NSO using satellite imagery from the Pléiades Neo, SuperView NEO-1, and SuperView 1 satellites.

Data Type	**Spatial resolution / Band count**
Superview NEO-1	30cm / RGB + Infrared
Airborne	10cm / RGB
Superview - 1	50cm / RGB
Pleidaes neo	30cm/RGB
LiDAR	(N.a)

Table 2 Overview of used Data type and its respective spatial resolution/Band count

Two photos were obtained for the Geul region (2,3) from the SuperView NEO-1 satellite, a constellation of very high-resolution optical satellites. These pictures, taken on May 27 and March 2, 2023, provide valuable

information. The first Image served as ground truth data, enabling the validation of classification results. The second Image was beneficial for evaluating the efficacy of the classification algorithm for mowed knotweed during the inactive winter season.

The SuperView NEO satellite instruments measure in a panchromatic band (resolution 0.3 meters) and in 4 different multispectral bands (resolution 1.2 meters):

- PAN: 450 - 890 nm (Panchromatic)
- B1: 450 - 520 nm (Blue)
- B2: 520 - 590 nm (Green)
- B3: 630 - 690 nm (Red)
- B4: 770 - 890 nm (NIR)

The Pléiades Neo satellite also provided a photo of the urban region. These high-resolution views of the research region from the pictures taken on April 6, 2023, made identifying and analyzing Japanese knotweed and other land cover elements easier. The French Pléiades NEO constellation consists of two identical satellites: Péiades NEO 3 and 4. The satellites have an instrument on board that measures in the panchromatic band (resolution 30 centimeters) and multispectral (resolution 1.2 meters) in 6 different bands:

- P: 450 - 800 nm (Panchromatic)
- B1: 400 - 450 nm (Deep Blue)
- B2: 450 - 520 nm (Blue)
- B3: 530 - 590 nm (Green)
- B4: 620 - 690 nm (Red)
- B5: 700 - 750 nm (Red Edge)
- B6: 770 - 880 nm (NIR)

SuperView-1 satellite pictures were used to depict the riparian area. These 0.5-meter-resolution photos, taken over four years(24), provide temporal information about changes in the land cover and the growth patterns of Japanese knotweed. Even though this dataset lacked validation data, it was critical in assessing the spatial distribution of Japanese knotweed.

The publisher of the Superview-NEO, Pleiades-NEO, and Superview-1 images in the Netherlands, Netherlands Space Office (NSO), provides context on the preprocessing that is performed and the same for the satellite images (NSO). The raw satellite photos were initially calibrated radiometrically. The next step included Sensor correction and, finally, orthorectified.

The riparian region of Geul has access to recent Light Detection and Ranging (LiDAR) scans, and the organization Rijkswaterstaat performed an additional scan of the area for their monitoring of the Maas River (Rijkswaterstaat, 2022). The metadata of the company scan reveals that the provided LiDAR measurement has a resolution of 16.6 points per square meter. These scans offered precise elevation and topography data that could be used as additional features to potentially improve the classification algorithm's accuracy by extracting CHM from the point cloud. The study's goal using LiDAR data was to increase the ability to distinguish between tall trees and Japanese knotweed, ultimately improving the effectiveness of the classification process overall. (Hick, 2021)

Airborne photos were gathered (4,5) for the riparian and urban areas of interest to enhance the study further. These photos were taken in 2022 and featured stereoscopic photos with a resolution of 10 cm and high-quality images taken during the season without leaves. The 10-centimeter ground pixel resolution ortho-photomosaics created from these photos enabled an inspection of the study areas where Japanese knotweed had been removed or cut. These photographs were used as training data to test the algorithm's

performance in identifying Japanese knotweed when mowed; (Beeldmateriaal, 2022) where the data was collected, gathers imagery twice a year, and they did not provide a specific preprocessing level of these products.

2.1 VALIDATION DATA

Two field visits were taken to collect real-world data as part of the validation process to inspect the classification model's performance and accuracy. Only two areas of interest were covered once during the data collection due to the study's 10-week time limit. However, observing the study sites more regularly throughout the data collection process and making field trips per year would prove helpful (van Iersel et al., 2018), especially now with higher resolution open data available for better research.(Nininahazwe et al., 2023)

Riparian area

The first location of interest was the mouth of the River Geul by Bunde in the Province of Limburg, located at 5.7151063E and 50.9080349N. This vegetation area variation in the classification analysis context represents riparian environment characteristics. On June 1, 2023, fieldwork was conducted, yielding the collection of 12 Japanese knotweed reference plots, which were afterward divided into additional samples based on the plant's shape. Some reference plots had more than just one Japanese knotweed present, but due to varying shapes of the IAS, they were collected as one sample and later split where different plants started overlapping.

Reference plot 1 Geul area

Urban area

The second point of importance is located in Neuiwegein, in the province of Utrecht, at 5.1101794E 52.0522948N. Twenty samples of Japanese knotweed were collected due to this fieldwork, which was done on June 13, 2023. They were later used as ground truth data to train an image from April 6, 2023. The threat to environmental diversity is worsened by alien invasive species in cities where there already are other invasive species (Štajerová et al., 2018)

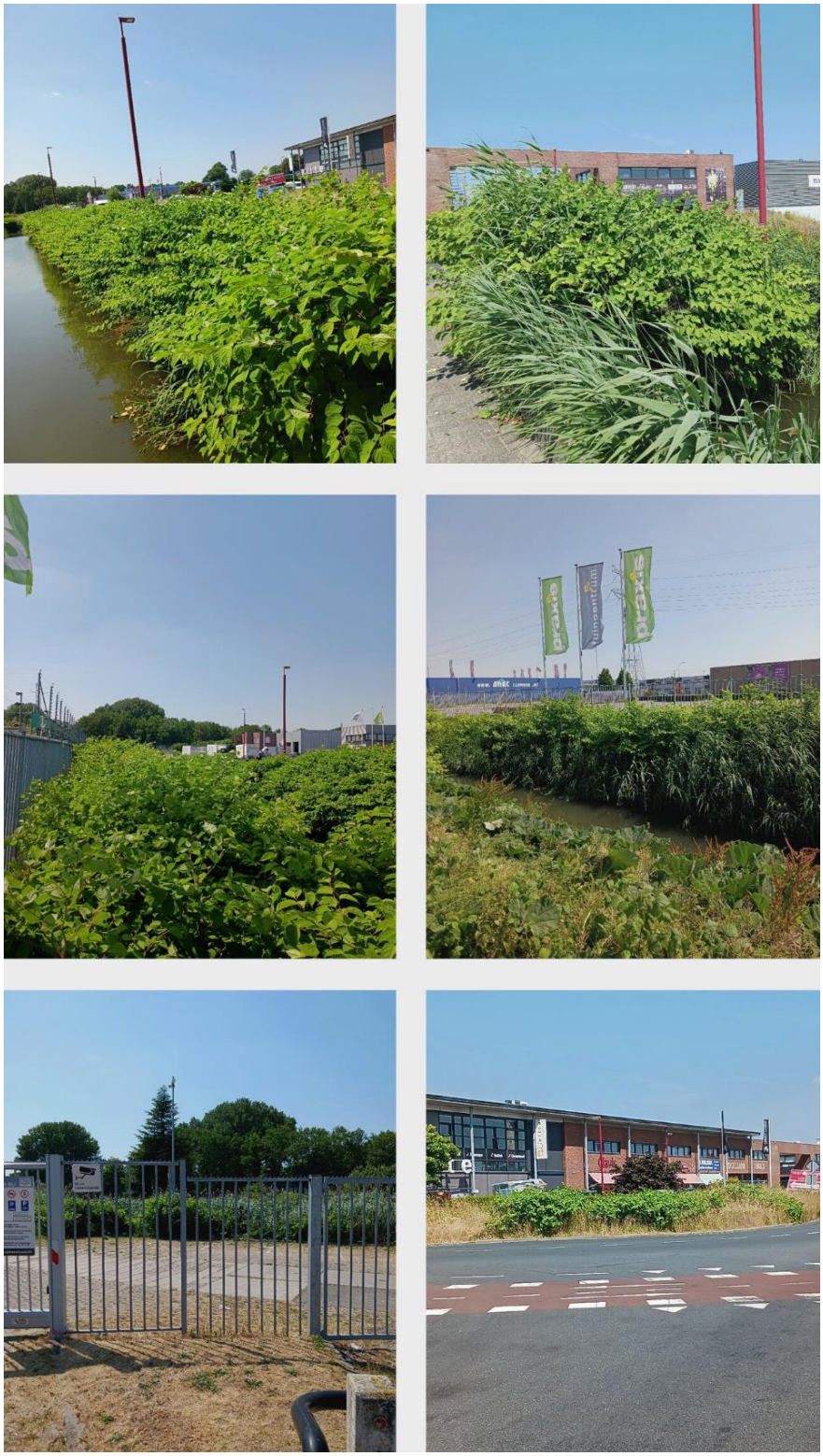

Reference plot 2 Nieuwegein area

Mowed Japanese knotweed

Even though only a few studied objects were collected after mowing, they were valuable as validation data. In the images, we can see mowed Japanese Knotweed; this data was used to confirm the removal process of IAS. By comparing the Image a few days before fieldwork that contains live knotweed and an image after the fieldwork, it is safe to assume that this knotweed is mowed from time to time, assuring us that we can identify it back in time. Which is later proved at (24) temporal analysis.

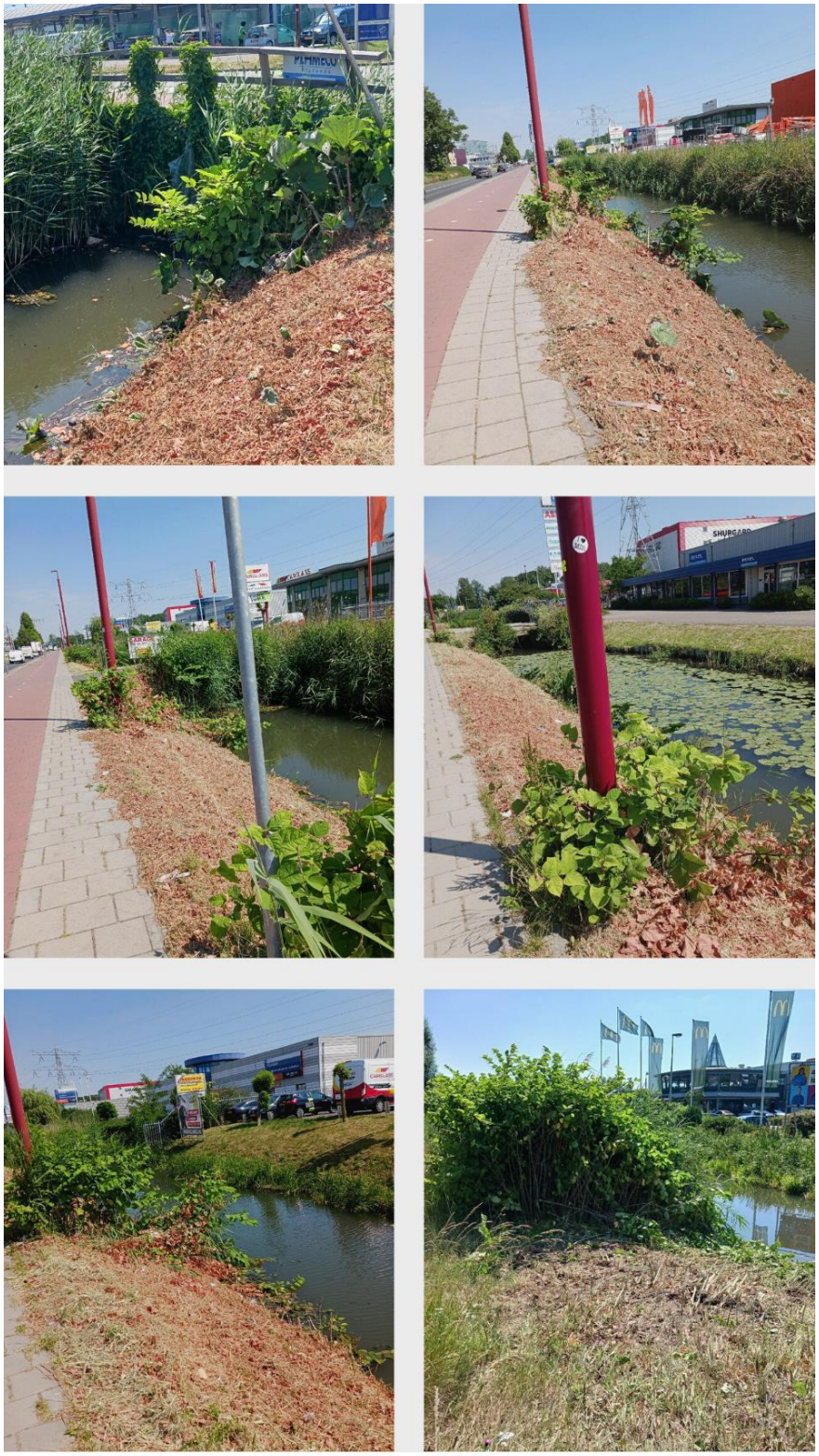

Reference Plot 3 Nieuwegein area Mowed knotweed

3 METHODOLOGY

The vegetation classification in this study was done using a complex process combining supervised machine learning models that apply pixel- and object-based techniques. This strategy enables comparing and evaluating each method's outcomes while considering their benefits and drawbacks.

Overall, this research methodology uses a combination of satellite imagery, airborne imagery, two distinct image analysis approaches, ground truth data, and different machine learning classification algorithms to shed light on the existence and growth patterns of Japanese knotweed in urban and riparian settings. In addition, the study utilizes the available validation data and combines additional information from LiDAR scans together with NDVI indices (Schenk et al., 2002)

The study aims to contribute to the comprehension and management of Japanese knotweed and other vegetation types within the study regions by assessing the classification results and considering the disadvantages and benefits of each approach and how they can be merged together for future analysis (Hick, 2021)

3.1 PIXEL VS OBJECT BASED APPROACH

The object-based approach is used in remote sensing and image analysis to extract information from imagery based on objects or regions rather than individual pixels. It involves grouping pixels together to form meaningful objects or segments, which are then analyzed and classified based on their characteristics (Liu et

al., 2010). In this respect, a group of pixels would serve as a training example for a classification algorithm, and the taught classification algorithm would then output a class prediction for pixels on a group basis. A simple example would be to divide an image into n segments of equal size and then assign a class (e.g., includes object/does not contain object) to each segment (Jones et al., 2011). Even though object-based classification is frequently employed in related research projects, it is crucial to recognize its shortcomings. The time-consuming and computationally demanding process of segmenting the training image into homogeneous objects is one of the major obstacles (Liu et al., 2010). Furthermore, the object-based classification may need to be more accurate since it is less likely to accurately capture the spectrum fluctuations inside particular objects (Liu et al., 2010)

Segmenting the items in the photos was another crucial step before performing object-based analysis. The ArcGIS Pro object-based analytic tools were used to do this segmentation operation as an example(6). Segmentation was used to create meaningful objects by combining pixels with comparable traits or attributes. This made it possible to separate certain features or items of interest, like vegetation patches or different land cover types, so that they could be easier examined and classified. The size and shape of the final segments were determined by several algorithms and parameters, including scale and shape variables, during the segmentation process (Jones et al., 2011). The study also takes into account the pixel-based technique in order to overcome these issues. The classification of pixels is done for each pixel, ignoring the values of pixels inside the locality and just using the spectral data available for that specific pixel. In this sense, each pixel would stand in for a training example for a classification algorithm, which would take the shape of an n-dimensional vector, where n was the number of spectral bands in the image data. As a result, each individual pixel in a picture would receive a class prediction from the taught classification algorithm. The accuracy of pixel-based classification may be slightly lower than that of object-based classification (Neupane et al., 2021). However, it performs more quickly, which is vital in the ArcGIS Pro environment. The study seeks to thoroughly evaluate the classification outcomes, considering both accuracy and efficiency, by comparing the findings of the two methodologies.

3.2 SAMPLES CLASS ASSIGNMENT

Two satellite photos of an urban and a riparian area are chosen as the primary training datasets. An important step to use them for classification is creating training samples due to the supervised process. Once the training samples are developed, the algorithm can learn on predefined classes and classify the rest of the Image. The usual approach is to set the train/test split values fixed. Arcigis Pro uses a predetermined split of 70/30, meaning that 70% of the provided samples are used for training, and the rest 30% are left out for testing.

For the class assignment, an approach was to implement the same amount of training samples per class. This assures that there is no class misbalance, and it is a known method when training models. Some classes, however, were much more sparse, with more pixels taken into the approach, then only half of the initial training samples were created for that class. Some of these more sparse classes are water, grass, buildings, and roads. The number of samples assigned to each classified Image varied. Training live knotweed classifier was conducted using 30 samples from the Nieuwegein area(1) and 17 from the Geul area(2). Mowed knotweed classification was performed using 22 training samples for each area(4,5). These plants can be visible better in this image (9). Combining Japanese knotweed samples with other classes resulted in a full training dataset. These datasets are then used to train two classification models using pixel- and object-based techniques.

3.3 CANOPY HEIGHT MODEL (CHM)

In addition, the study implements LiDAR scans starting from 2022 into the classification process, which is only accessible in riparian areas. Lidar (Light Detection and Ranging) is a remote sensing technology that measures distances and captures detailed information about the Earth's surface using laser pulses(Naeseet et al ., 2002). It provides precise and high-resolution data by emitting laser beams and measuring the time it takes for the laser to return after hitting an object. CHM has become a valuable tool in various fields, including forestry, geology, urban planning, and environmental monitoring (Hick, 2021).

In the context of this study, lidar data was utilized to extract height information, which serves as an additional input for the classification process. Height extraction from lidar data enables to capture of the vertical dimension of the study area, which can provide valuable insights into the structure and composition of the landscape. However, to rely on these data, a Canopy Height Model must first be created. Original data was stored in LAS format, which, when applied to ArcGIS, resulted in a point cloud(point cloud). With these specifics. Then two layers were extracted, the first point of return and the ground point of return. They respectively give information about the Digital elevation model and digital surface model. Using both layers in the raster calculator made it possible to subtract DEM from DSM, resulting in Canopy Height Model(11). This is how vegetation height is measured primarily in research (Naeseet et al ., 2002). The CHM was evaluated for the whole study area of Geul to distinguish how vegetation height varies. By incorporating height as a feature in the classification algorithm, the accuracy and reliability of the land cover classification can potentially be improved.

3.4 MACHINE LEARNING CLASSIFICATION ALGORITHMS

The study mainly concentrated on Support Vector Machine (SVM) and Random Trees (RT) classifiers. These classification algorithms employed are well-known machine learning algorithms utilized in remote sensing for applications of various problems, including vegetation classification. (Nininahzwe et al., 2023)

The supervised learning algorithm Support Vector Machine (SVM) can be used to solve problems involving binary and multiclass classification. (Yue et al., 2003) SVM aims to find the best hyperplane to divide many classes in a high-dimensional feature space. In order to determine the appropriate decision boundary that maximizes the margin between classes, it maps the input data into a higher-dimensional space. SVM can handle enormous feature sets and complicated, nonlinear classification problems. In this case, the dimension amount depends on the imagery used and if additional data was provided as input. Satellite images used four

spectral bands, whereas airborne images used three bands. This translates into 4 and 3, respectively, used dimensions for SVM, additional input, NDVI, and CHM increased dimensions value by 1. Thus the complexity of the dimensions varied from 3 to 5 depending on the specific case.

An ensemble learning technique called Random Trees (RT) mixes different decision trees to produce predictions. A distinct random subset of the training data and a random subset of characteristics are used to construct each tree in the forest. The Random Trees classification method is a supervised machine-learning classifier based on constructing many decision trees, choosing random subsets of variables for each tree, and using the most frequent tree output as the overall classification. High precision, scalability, and the capacity to manage datasets with many dimensions are characteristics of RT (Gislason et al., 2004)

3.5 PERFORMANCE ASSESSMENT METRICS

First, to start analyzing classification results in ArcGIS Pro, there must be accuracy assessment points. These are randomly created sample points for post-classification accuracy evaluation. For each classification process, 500 points were created and split equally for each class. This approach is called random balanced sampling and ensures a more fair and unbiased evaluation of the results for all classes by not discriminating against Japanese knotweed. Due to its small spatial resolution, more than proportional random sampling is needed. In images (12) and (13) we can see respectively for riparian and urban a process of creating training samples. The mowed knotweed distribution for training samples was performed this way(7,8). (Wu et al., 2014) The chosen amount of points could be better, as the classification evaluation is more accurate with a higher amount of points, reducing the division's randomness. The next step is to compare the post-classified Image with the pre-classified one and assign each accuracy assessment point a ground truth value. The process resulted in an attribute table with 500 points for each classification, contrasting the classified values with ground truth values. Overall 8000 points were evaluated by eye and assigned ground truth values to each class. This process allowed us to develop and examine performance assessment metrics by creating a confusion matrix. The accuracy of the user and producer for each class is calculated using this tool, along

with the overall kappa index of agreement. These accuracy percentages are 0 to 1, with one denoting perfect accuracy. An illustration of a confusion matrix is as follows:

		Actual Values	
		Positive (1)	Negative (0)
Predicted Values	Positive (1)	True Positive	False Positive
	Negative (0)	True Negative	False Negative

User Accuracy or precision and Producer accuracy or recall are commonly used metrics to assess the effectiveness and reliability of such models. These metrics provide insights into the model's ability to classify instances (Nininahzwe et al .,2023).

The user's accuracy reveals false positives or instances where pixels are wrongly assigned to a known class when they need to be. For instance, a pixel might be categorized as impervious in the classified Image yet be classified as a forest in the reference. According to the reference data, the impervious class has extra pixels that it should not have. Mistakes of commission, precision, or type 1 error are further terms for user accuracy. Formula for User accuracy is as follows:

Precision = (True Positive) / (True Positive + False Positive)

The table's rows are read for the information needed to calculate this error rate. The Total row displays the total number of points that should have been classified as belonging to a particular class based on the reference data.

A false negative produced by the producer occurs when pixels belonging to a known class are labeled as something else. As an illustration, consider a pixel labeled as a forest but actually impenetrable. According to the reference data, the impervious class, in this instance, has missing pixels. Errors of omission, recall, or

type 2 errors are other names for producer accuracy. The information needed to calculate this error rate is retrieved from the table's columns.

Formula for Producer accuracy is as follows:

Recall = (True Positive) / (True Positive + False Positive)

The Total column displays the total number of points that the categorized map classified as belonging to a particular class.

Knotweeds comprise a relatively small fraction of our study region; therefore, interpreting results from other classes could be inaccurate. This is because overall accuracy and kappa may not accurately reflect the performance of the classifier for the minority class because they are influenced by the dataset's dominant classes. Class-specific measurements are the primary focus (Martin et al., 2018). Because of this, evaluation criteria like kappa or total accuracy were excluded.

3.6 NDVI

In the context of this study, NDVI was employed as a critical component for vegetation classification. Similar to previous research (Hick, 2021), NDVI was utilized to extract valuable information about vegetation types in the study area. By calculating NDVI, researchers can derive additional insights about differences in vegetation health, density, and distribution, which can significantly aid in accurate and efficient classification. NDVI values range means how healthy the plant is, with -1 to 0 being a dead or inanimate object, 0 to 0.33 being a diseased plant, 0.33 to 0.66 means moderately healthy plant and 0.66 to 1 is a very healthy plant.

The formula for computing NDVI is:

NDVI = (NIR - Red) / (NIR + Red)

Where:

NIR (Near Infrared) is the spectral reflectance of the near-infrared band.

Red is the spectral reflectance of the red band.

This formula utilizes the difference and sum of reflectance values from the near-infrared and red bands to create an index that highlights vegetation.

For the sake of Arcgis pro and analysis, the values were moved from -1/1 to 0/2 and multiplied by 1000 to make it as close as possible to reflecting floating points by integers.

By incorporating NDVI into the classification process (Jones et al., 2011), one can enhance the accuracy of land cover mapping and distinguish between different vegetation classes more effectively.

Even though it seems futile to distinguish Japanese knotweed using pure NDVI values for now, current research has shown a minimal increase in classification accuracy when NDVI is included in the machine learning process. This project additionally aimed at comparing NDVI values through temporal analysis as an invitation for the complete study, In order to distinguish Japanese knotweed and values for its regrowth phase. The additional information provided by NDVI (Hick, 2021) can potentially help in understanding vegetation's spatial distribution and health.

3.7 TEMPORAL ANALYSIS

As mentioned in Section 1, classifying mowed Japanese knotweed requires up to certain assumptions. In addition to the recent ground truth data, both sites of interest had a series of images collected, ranging back to 2019. The first aim of this approach was to compare if the supposed mowed knotweed is valid by comparing the airborne images with previous data. The result of this assumption is shown here to allow for later analysis of the mowed knotweed by having reference data. As it is clear, comparing an image from x with x allows us to determine that the mowed plant is Japanese knotweed and can be classified. The second use of temporal analysis was in evaluating NDVI values, twice during the spring season(2,25) and once in winter(3). A visual

assessment was also undertaken to see how the IAS of interest spatial distribution changed throughout the last few years(24). Despite the lack of ground truth data for this temporal period, the results can still be quite insightful when viewed under the abovementioned restrictions. These photos are divided into four seasons.

3.8 PREPROCESSING

As mentioned in Section 1, The satellite pictures used in this work underwent several critical processes throughout the preprocessing phase to guarantee the highest data quality and enable the analysis. In addition, extra preprocessing was applied to increase the data quality.

First, to focus the analysis on the particular study location, all photos were clipped to include the area of interest(1). This reduced computational needs by defining the intended extent using a polygon. The photos were then improved by going from an 8-bit to a 64-bit bit depth. This improvement was made to handle the detailed spectral data in the photos and facilitate a more accurate and in-depth analysis. The ability to distinguish between minute fluctuations in pixel brightness and spectral features would be improved by expanding the bit depth of the images.

When evaluating CHM derived from LiDAR, extracting return signals for the point cloud is the first step. First point and ground point returns were then subtracted from each other, resulting in the canopy height model. The formula was applied to obtain NDVI values, Both of these operations were performed in a raster calculator.

The preparation stage ensured the satellite photos were prepared for further analysis via object-based segmenting(6), boosting their bit depth, and cropping the images to the area of interest. These procedures improved the data quality, made it easier to extract pertinent objects, and laid the groundwork for a precise and thorough object-based analysis in this vegetation classification.

4 RESULTS

Results This study aimed to compare the performance of various categorization techniques for finding mowed Japanese knotweed in Utrecht and the mouth of the De Geul rivers. Airborne photos, satellite images, lidar data, and auxiliary datasets, including the Normalized Difference Vegetation Index (NDVI), were all used in the investigation.

Classification of Japanese knotweed: Overall accuracy assessment is portrayed in 3 tables . The first shows the classification results using the user accuracy metric[1]. The second table has the classification results per producer accuracy metric[2]. The final table[3] summarizes the performance per image analysis approach and machine learning classification algorithm for both metrics.

User Accuracy Assessment of Geul and Nieuwegein Area, for Mowed and Live Japanese Knotweed using SVM and Random Trees Models Through Object-Based and Pixel-Based Approaches							
Geul area	**Object-Based Approach Average**	**SVM Model**	**RT Model**	**Pixel-Based Approach Average**	**SVM Model**	**RT Model**	**Average User Accuracy**
Live Knotweed	29.5%	35%	24%	20.5%	24%	17%	25%
Mowed Knotweed	21%	26%	16%	15%	15%	15%	18%
Nieuwegein area	**Object-Based Approach Average**	**SVM Model**	**RT Model**	**Pixel-Based Approach Average**	**SVM Model**	**RT Model**	**Average User Accuracy**
Live Knotweed	48%	49%	47%	39.5%	46%	33%	44%
Mowed Knotweed	24.5%	26%	23%	14.5%	14%	15%	19.5%
Average User Accuracy	30.75%	34%	27.5%	22.375%	24.75%	20%	26.25%

for both locations							

This paper's highest Average User accuracy or precision value is equal to 26.25%. Live knotweed has a higher classification percentage compared to mowed knotweed. Its average accuracy is 34.5%, whereas it is 18.75% for mowed knotweed. In the context of Japanese knotweed classification, the Object-based image analysis proved to be more accurate, reaching an average of 30.75%, compared to the Pixel-based image analysis, which averaged 22.375% overall. Regarding the machine learning classification algorithm, the SVM is proven to perform better with this task. This model's average accuracy is 29.38%, and the RT performance is 23.75%. The urban area of Nieuwegein was easier to identify in terms of Japanese knotweed; its average accuracy for both life and mowed knotweed is 31.75%, whereas the riparian area of Geul averaged 21.5% user accuracy.

Producer Accuracy Assessment of Geul and Nieuwegein Area, for Mowed and Live Japanese Knotweed using SVM and Random Trees Models Through Object-Based and Pixel-Based Approaches							
Geul area	**Object-Based Approach Average**	**SVM Model**	**RT Model**	**Pixel-Based Approach Average**	**SVM Model**	**RT Model**	**Average Producer Accuracy**
Live Knotweed	98%	96%	100%	94.5%	89%	100%	96.25%
Mowed Knotweed	100%	100%	100%	91.5%	83%	100%	95.75%
Nieuwegein area	**Object-Based Approach Average**	**SVM Model**	**RT Model**	**Pixel-Based Approach Average**	**SVM Model**	**RT Model**	**Average Producer Accuracy**
Live Knotweed	90%	92%	88%	81%	85%	77%	85.5%

Mowed Knotweed	88.5%	100%	77%	87%	74%	100%	87.75%
Average Producer Accuracy for both locations	94.125%	97%	91.25%	88.5%	82.75%	94.25%	91.31%

The highest Average Producer accuracy or recall value that this paper achieved is equal to 91.31%. Live knotweed has a higher classification percentage compared to mowed knotweed. Its average recall is 90.875%, whereas it is 91.75% for mowed knotweed. In the context of Japanese knotweed classification, the Object-based image analysis proved to be more accurate, reaching an average of 94.125%, compared to the Pixel-based image analysis, which averaged 88.5% overall. Regarding the machine learning classification algorithm, the SVM is proven to perform better with this task. This model's average accuracy is 89.875%, and the RT performance is 92.75%. The urban area of Nieuwegein was easier to identify in terms of Japanese knotweed; its average accuracy for both live and mowed knotweed is 86.625%, whereas the riparian area of Geul averaged 96% producer accuracy.

User and Producer Accuracy Assessment of Geul and Nieuwegein Area, for Mowed and Live Japanese Knotweed using SVM and Random Trees Models Through Object-Based and Pixel-Based Approaches							
Geul area	**Object-Based Approach Average**	**SVM Model**	**RT Model**	**Pixel-Based Approach Average**	**SVM Model**	**RT Model**	**Average difference in Accuracy per model**
User accuracy	25.25%	30.5%	20%	17.75%	19.5%	16%	7%
Producer accuracy	99%	98%	100%	93%	86%	100%	-8%
Nieuwegein area	**Object-Based Approach Average**	**SVM Model**	**RT Model**	**Pixel-Based Approach Average**	**SVM Model**	**RT Model**	**Average difference in Accuracy per model**
User accuracy	36.25%	37.5%	35%	27%	30%	24%	3.75%

Producer Accurcy	89.25%	96%	82.5%	84%	79.5%	88.5	2.25%

When comparing final values per model, it is pretty clear how different their performance is. SVM has an average higher accuracy over all instances. It is interesting to see how Pixel-based image analysis performs better with type 2 error. These small differences can however be attributed to randomness.

Lidar Data Incorporation: Lidar data was incorporated into the classification system to improve the separation of Japanese knotweed and other land cover classes. However, the findings demonstrated that the impact of lidar data on accuracy did not improve the classification. As shown in this Image, the performance of both machine learning algorithms did not improve.[19,20] There are minor pixel placement changes; however, these were mostly about other classes. In this example, amount of trees is reduced, and shrubs are less spread out; this is more accurate for these classes when looking at ground truth data. Japanese knotweed pixel placement has not changed. Implying no direct improvement of classification in this case. Only Pixel-based image analysis allowed for additional input of these types in ArcGIS Pro; thus, OBIA was not performed.

Incorporation of NDVI: Including NDVI as additional input for satellite images from the region of interest aimed to leverage spectral information and vegetation density metrics for improved classification accuracy. Calculating NDVI per class was done by tabulating an area and adding additional statistical measures. When added as an extra dimension to the classification process, the performance of the models did not improve, as shown in [19.21]. The NDVI values for Japanese knotweed ranged from similar to grass and shrubs; trees had higher values. Comparing values for different vegetation seasons showed that when alive, the NDVI mean value is around 1327; for the winter season, when knotweed was mowed, the mean is around 879.

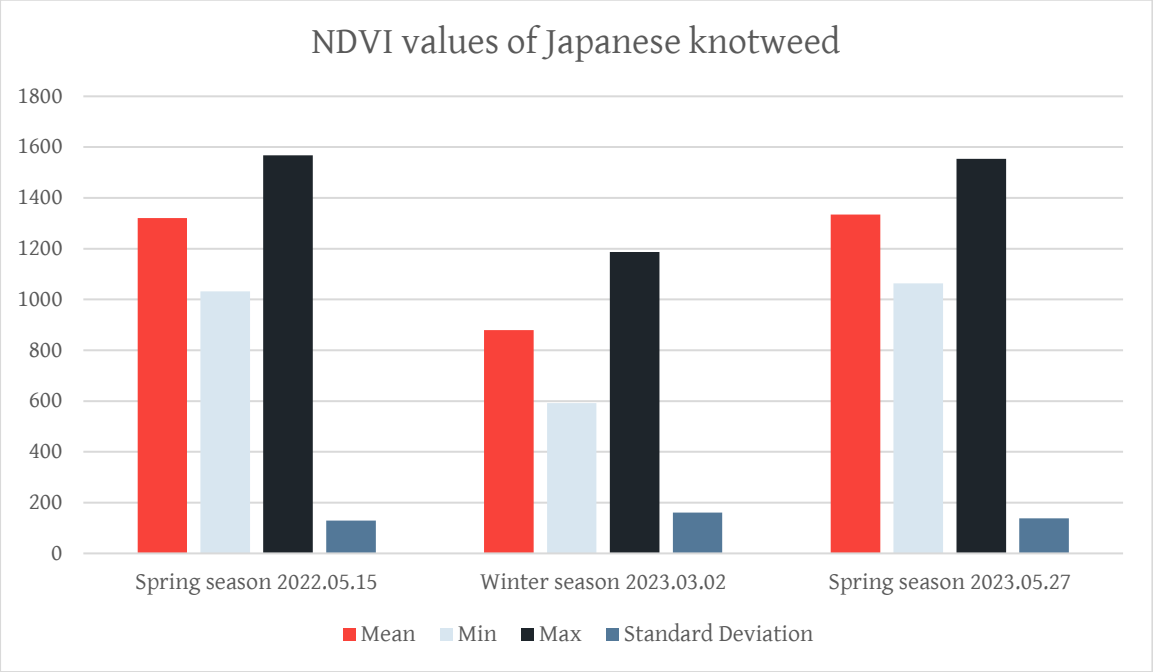

When looking at the minimal and maximal values for both spring seasons, one can see that they are barely different. Comparing Japanese knotweed to other classes, that is, shrubs, trees, grass, and other vegetation, shows that most classes have similar results. (16,17,18)Trees and shrubs were most representative of knotweed, as they got comparable values across all the computed statistics. However, the mean for the mowed Japanese knotweed is quite different from other classes, showing how the values range when dealing with no vegetation season.

Temporal analysis

When comparing images from 2022.05.15(25), 2023.03.02(3), and 2023.05.27(2), the Japanese knotweed has been present in the area already since 2022.05.15. This allows us to classify mowed knotweed from 2022 using aerial imagery and extract NDVI values per season. Earlier data from 2019, as shown in (24) still has the IAS

present. Japanese knotweed is only partially visible in these pictures, showing how quickly it can spread there.

5 DISCUSSION

The findings of this study showed that different remote sensors / data types and processing techniques had varying degrees of accuracy in classifying and identifying alive Japanese knotweed, Average of 26.25% User accuracy or precision and 91.30% of Producer accuracy or recall. Results varied per study site, but we are primarily interested in user accuracy as its accurate map representation. There is a clearly better performance in urban areas, 31.75%, both for live 44% and mowed knotweed 19.5%. This can be accumulated to less diverse vegetation; also, it is possibly different due to a higher amount of training samples compared to riparian areas or to examine the Image in IRG bands. The study site of Geul averaged 21.5% user accuracy, precisely 25% for life and 18% for mowed knotweed. More dynamic riparian areas proved to be a more challenging task for the analysis. However, it provided valuable information through CHM usage. This input proved insignificant in the classification task for Japanese knotweed but improved the accuracy for other classes(19,20). This makes sense as the LiDAR scan is from the year 2022 and primarily includes detailed point clouds for trees and shrubs compared to Japanese knotweed as seen in (10). It's clear that the knotweed is barely represented by the scan; only the edges of the plant by water are registered. This shows how crucial proper temporal data incorporation is; if the scan was performed during the season when Japanese knotweed was fully present, one could apply a threshold to specifically look for Japanese knotweed class besides shrubs as (Hick, 2021) did. However, a different CHM model could be derived not from LiDAR(Jones et al., 2011). Values for CHM help identify other classes, with a mean of 482 shrubs, trees 1366, and another veg 108; they need a better representation of Japanese knotweed to be helpful as a benchmark in future research. NDVI

values incorporation also did not improve the classification as shown in (19, 21); This is more of a surprising result looking at previous research (Hick, 2021 & Dorigo et al., 2012) that used NDVI effectively. The reasoning for that is not exactly sure; it can be due to lower spectral resolution than other studies (Hick, 2021 & Dorigo et al., 2012) or not applying thresholds to and values. The NDVI values per season varied considerably; the spring period was similar in both years, while the winter season, when knotweed was mowed, had a mean of 879, while the max value reached 1187. This indicates that the NDVI values are different per sample and allows us to assume that it can be possible to distinguish Japanese knotweed using NDVI during the regrowth process. Suppose its max values range from 1686 to 1187 during different year seasons. In that case, they could be potentially classified using purely NDVI values if the surrounding environment is not growing as fast. this observation was allowed by the temporal analysis with Superview – 1. One could examine the temporal resolution of the Japanese knotweed regrowth process more thoroughly and try to answer if it is possible to accurately identify JK using both mowed and live data samples. More research should be undertaken on NDVI reflectance of Japanese knotweed; more specifically, it's advised to use different software with more adjustable parameters. When using Python, for example, sci-kit learn, it is possible to preprocess the NDVI layer more accurately than ArcGIS Pro. This allows for more adjustments in the usage of NDVI.

Classifying specific invasive species based on height, color, and spatial variation is a complex task; looking at previous studies, previous research had mixed results in performance. A lot can be accounted for sensor and data quality. Compared to peers, this study has average results, being lower in most cases. (Martin et al., 2018) Looking at satellite results, Pleidas obtained a higher result of 49% being in a similar environment. This is promising, looking at time constraints related to this study. Superview NEO's results are worse than its previous satellite; this can be attributed to different reasons. For example, Pleiades was evaluated in urban areas with less homogenous environments and higher distribution of buildings and roads with high precision making it easier to classify JK. Although airborne imaging offers high-resolution photos and extensive information (Michez et al., 2016), the accuracy was moderate for detecting mowed knotweed 18.75% . This shows that additional development is required to improve the precision of airborne imagery-based

classification algorithms. When looking at previous research findings, the Airborne and UAV are comparably higher than our results (Dorigo et al., 2012). This can be mainly attributed to slightly different tasks; classifying mowed knotweed is significantly more complicated as it mainly stems, and Japanese Knotweed has hollow stems.

Previous research used different machine learning models and image analysis processes; Here, they were both tested to evaluate the performance of SVM, RT models, and OBIA together with PBIA approaches. Previous research mainly used RF (Michez et al., 2016), but even then, the SVM performed better in every case, outperforming RT by 5.25% on average in our case. The SVM method outperformed other algorithm (22,26) in handling complicated datasets and generating optimal decision boundaries. It is important to remember that the RT model still produced acceptable outcomes and can represent a good option, depending on the classification objectives and dataset features. However, this is very case-specific, and once a study is conducted where one model outperforms different by a lot, there is no dominating difference between these two.

Additionally, one can explore neural networks (Nininahzew et al., 2023) and other classifiers that average high results. As expected, the OBIA proved to be more reliable for identifying Japanese knotweed(22,19), having an average user accuracy of 30.75% compared to PBIA's 22.375%. This shows how vital spatial analysis is in the vegetation classification process. OBIA should be a preferred approach; its higher accuracy was shown in a previous study (Liu et al., 2010). One could compare the results of both approaches on a larger scale, where computation processing matters more, and look at how much time can be optimized using PBIA in the performance price. In addition, an increase in the accuracy sample size would be beneficial; this will ensure that there can be a more robust distribution of accuracy assessment points. Thus leading to more unbiased results.

New management strategies, such as introducing biological agents like fleas[42] or pigs, appear promising. However, these strategies take a long time to prove they are effective, and looking at the Temporal analysis, it is clear that Japanese knotweed grows rapidly. It still needs to be improved how monitoring of IAS, but one should control the region to notice when new plants are growing. Further enhancing classification accuracy

might be the exploration of metrics like the Leaf Area Index (LAI) by collecting temporally or angularly spread data. Reducing temporal inconsistencies and improving the classification findings' accuracy can be achieved by collecting validation data in the same month as the data sources. Analysis of previous temporal images from SuperView-1 allowed us to identify and use Japanese knotweed to classify mowed knotweed. The classification is robust with this assurance, as one always needs validation data in this process. However, in both the Utrecht and the mouth of De Geul regions, satellite imaging proved to be a more reliable method for spotting Japanese knotweed compared to airborne imagery. When faced with increasing erosion and flooding threats, the Japanese knotweed needs to be monitored better, and more innovative approaches should soar to deal with this species. (Colleran et al., 2020). It's suggested to look more into the Japanese knotweed erosion rate (Aguilera et al., 2010; Collingham et al., 2000; DAISIE, 2008; Smith et al., 2007). As this claim makes both WFD and UE directives (European Commission., 2019) focused on identifying Japanese knotweed in riparian areas.

Future research should concentrate on gathering ground truth data at various time points and creating sophisticated temporal analytic approaches to capture the rapid pattern of the Japanese knotweed growth process to alleviate this shortcoming. Even when improperly mowed, the plant of interest is easily identifiable due to its natural size and stem features. This brings up another problem with the poorly handled procedure; if this invasive species is not adequately managed, it will simply spread through the water. This situation proves even more, how crucial it is to monitor this plant (Rouleau et al., 2023)

6 CONCLUSION

This study aimed to assess if remote sensing can be used to accurately classify Japanese knotweed in urban and riparian areas, an invasive alien species that is of interest to UE (European Commission, 2019) directive. Research proved that while it is possible to classify JK with moderate user accuracy of 49% in urban areas and

35% in riparian areas (23,22), it is not a practical approach to rely on field operations yet. Technological advancement allows more advanced data types, like hyperspectral data, can be used.

This research analysis implies that combining pixels into objects and considering spatial relationships improves classification accuracy(22,19). An object-based analysis is beneficial when dealing with complicated plant patterns and mixed land cover types since it can more accurately reflect the variety within objects.
The different machine learning performances compared to show how the Support Vector machine model does better against Japanese knotweed classification than the Random Trees model(22,26). Proving to be a more reliable approach when dealing with multidimensional data; however, more tests and parameter adjustments should be made before saying this confidently.

Overall, the research's findings offer insightful, helpful information for creating precise algorithms for Japanese knotweed detection. The outcomes show the potential of airborne and satellite data for classifying vegetation while also hinting at certain benefits of object-based analysis over pixel-based methods. Even though adding lidar data and NDVI did not improve Japanese knotweed classification accuracy, the prediction accuracy was higher for other classes, and more research may look into alternative techniques and data sources to increase performance on plant of interest.

Classification of mowed Japanese knotweed proved to be a hard task, reaching the highest accuracy of 18% in riparian and 19.5% in urban areas (22,23). As a new approach, it made sense to be unsuccessful. However, it can be used as a future research direction. Due to Japanese knotweed's rapid growth and damaging impacts on soil erosion make it a severe environmental threat. Close observation is suggested in riparian regions, especially where knotweed has more opportunities to spread; this could allow a more effective map of the regrowth process of the invasive alien species. Where waterboards want to decrease soil erosion to control

the effects of this invasive species. Japanese knotweed can grow beneath concrete tiles in urban environments, further complicating eradication efforts.

The methods utilized in this study need to be improved before they can be relied upon entirely, even though they can be used to advance research further and emphasize the monitoring of invasive alien species. The chosen cutoff for accuracy evaluation metrics will vary depending on the task. However, with more frequent temporal analysis in the future, it may be possible to digitize the process to a certain extent and lessen the amount of fieldwork required.

Even though this study had some drawbacks, such as time, software, and fieldwork restrictions, the outcomes were encouraging. The classification algorithm created in this study must be further improved as it has yet to attain the operational dependence level.

It is advised to gather more validation data from urban and riparian locations to improve future studies. This will offer chances to evaluate the algorithm's performance in various environmental scenarios, increase accuracy, and test it on previously uncovered data.

We can lessen Japanese knotweed's negative environmental consequences, protect plant diversity, and guarantee the long-term sustainability of ecosystems by tackling its expansion and putting robust mapping and measures in place.

6.1 FUTURE WORK

Future Research: Several directions might be taken to improve the precision and efficacy of Japanese knotweed monitoring and classification using remote sensing techniques. The following ideas can direct additional study and advancements in this area:

1. Obtain hyperspectral data with high spatial resolution. Hyperspectral data were considered to be used in this investigation. However, categorizing tiny flora like Japanese knotweed was difficult, with a resolution of

30 meters per pixel. More accurate identification and classification of invasive species will be possible by acquiring hyperspectral data with higher spatial resolution.

3. Investigate alternative software and automation: Although Python was utilized in this study, other software tools, such as ArcGIS Pro, can offer more flexibility and automation options. The categorization process can be improved even more, and model parameters can be optimized by creating customized scripts or employing deep learning techniques.

4. Obtain airborne photos of Japanese knotweed that are currently growing: Using airborne photography that is primarily targeted at Japanese knotweed that is currently growing can offer more accurate and current information on the growth patterns and geographic distribution of the invasive species. Airborne imaging enables more significant differentiation between plant classifications and can capture finer details.

5. Develop a shadow classifier to reduce the misclassification of the model in shade areas.

Long-term Recommendations

Take into account the following ideas for long-term improvements in Japanese knotweed monitoring and management:

1. Consider extra environmental factors: Japanese knotweed's phenological characteristics, precipitation, temperature, and other environmental elements can all be considered to understand how the plant behaves and grows. Methods like complete introspection. These parameters can be measured and examined using chemometric techniques, and Fourier transform infrared spectroscopy.
2. Increase the accessibility of ground truth data: Accurate classification algorithms depend on collecting more ground truth data. Monitoring the same areas for an extended time while collecting validation data all year will improve classification accuracy and offer valuable insights into temporal changes.

6.2 LIMITATIONS:

Despite the insightful conclusions drawn from this study, some shortcomings should be acknowledged:

1. Use of ArcGIS Pro: The analysis is constrained in several ways by using ArcGIS Pro, especially in terms of computational power, machine learning settings, and processing speed. Future projects should look into and use external software solutions that provide more flexibility and sophisticated functionality.
2. Time limitations: This project's two-month time frame limited the quantity of validation data that could be gathered and the scope of the coding and analysis that could be done. Similar analyses over a longer time frame would allow for a more thorough assessment and improve the temporal study of Japanese knotweed dynamics
3. Varying conditions in satellite photos: Some satellite images utilized in the study had varying lighting, impacting classification performance. The accuracy and consistency of classification results would be improved by addressing these temporal image differences utilizing cutting-edge image processing techniques.
4. Lidar data limitations: When deriving a new CHM, it is advisable to include it during Japanese knotweed vegetation season.

7 REFERENCES

1. Asner, G. P., Jones, M. O., Martin, R. E., Knapp, D. E., & Hughes, R. F. (2008). Remote Sensing of Native and Invasive Species in Hawaiian Forests. Remote Sensing of Environment, 112(5), 1912-1926.
2. Beeldmateriaal (2018) Over Beeldmateriaal | Beeldmateriaal Nederland
3. Benediktsson, J. A., & Sveinsson, J. R. (1997). Feature Extraction for Multisource Data Classification with Artificial Neural Networks. International Journal of Remote Sensing, 18(4), 727-740.

4. Bradford, M. A., Schumacher, H. B., Catovsky, S., Eggers, T., Newingtion, J. E., & Tordoff, G. M. (2007). Impacts of Invasive Plant Species on Riparian Plant Assemblages: Interactions with Elevated Atmospheric Carbon Dioxide and Nitrogen Deposition. Oecologia, 152, 791-803.
5. Colleran, B., Lacy, S. N., & Retamal, M. R. (2020). Invasive Japanese knotweed (Reynoutria japonica Houtt.) and related knotweeds as catalysts for streambank erosion. River Research and Applications, 36(9), 1962-1969.
6. Collingham, Y. C., Wadsworth, R. A., Huntley, B., & Hulme, P. E. (2000). Predicting the Spatial Distribution of Non-Indigenous Riparian Weeds: Issues of Spatial Scale and Extent. Journal of Applied Ecology, 37, 13-27.
7. Conolly, A. P. (1977). The Distribution and History in the British Isles of Some Alien Species of Polygonum and Reynoutria. Watsonia, 11, 291-311.
8. Dash, J. P., Watt, M. S., Paul, T. S., Morgenroth, J., & Pearse, G. D. (2019). Early Detection of Invasive Exotic Trees Using UAV and Manned Aircraft Multispectral and LiDAR Data. Remote Sensing, 11(15), 1812.
9. Dorigo, W., Lucieer, A., Podobnikar, T., & Čarni, A. (2012). Mapping Invasive Fallopia Japonica by Combined Spectral, Spatial, and Temporal Analysis of Digital Orthophotos. International Journal of Applied Earth Observation and Geoinformation, 19, 185-195.
10. European Commission (2019), The European Green Deal, Communication from the Commission to the European Parliament, the European Council, the Council, the European Economic And Social Committee and the Committee of the Regions, COM(2019) 640 final, https://eur-lex.europa.eu/legal-content/EN/TXT/?uri=CELEX%3A52019DC0640
11. Hick, D. (2021). Development of a Remote Sensing Solution to Map Invasive Plant Species [Poster].
12. Hulme, P. E., Nentwig, W., Pyšek, P., & Vilà, M. (2010). DAISIE: Delivering Alien Invasive Species Inventories for Europe.

13. Council, I. U. C. N. (2000, February). Guidelines for the prevention of biodiversity loss caused by alien invasive species. In Prepared by the IUCN/ SSC Invasive Species Specialist Group (ISSG) and approved by the 51st Meeting of the IUCN Council, Gland Switzerland..
14. Jones, D., Pike, S., Thomas, M., & Murphy, D. (2011). Object-based Image Analysis for Detection of Japanese Knotweed Sl taxa (Polygonaceae) in Wales (UK). Remote Sensing, 3(2), 319-342.
15. Jombo, S., Adam, E., & Odindi, J. (2021). Classification of Tree Species in a Heterogeneous Urban Environment Using Object-Based Ensemble Analysis and World View-2 Satellite Imagery. Applied Geomatics, 13(3), 373-387.
16. Kowarik, I. (2008). On the Role of Alien Species in Urban Flora and Vegetation. Urban Ecology: An International Perspective on the Interaction between Humans and Nature, 321-338.
17. Lawrence, R. L., Wood, S. D., & Sheley, R. L. (2006). Mapping Invasive Plants Using Hyperspectral Imagery and Breiman Cutler Classifications (randomForest). Remote Sensing of Environment, 100(3), 356-362.
18. Lass, L. W., Prather, T. S., Glenn, N. F., Weber, K. T., Mundt, J. T., & Pettingill, J. (2005). A Review of Remote Sensing of Invasive Weeds and Example of the Early Detection of Spotted Knapweed (Centaurea Maculosa) and Babysbreath (Gypsophila Paniculata) with a Hyperspectral Sensor. Weed Science, 53(2), 242-251.
19. Liu, D., & Xia, F. (2010). Assessing object-based classification: advantages and limitations. Remote sensing letters, 1(4), 187-194.
20. Lu, D., & Weng, Q. (2007). A Survey of Image Classification Methods and Techniques for Improving Classification Performance. International Journal of Remote Sensing, 28(5), 823-870.
21. Martin, F. M., Müllerová, J., Borgniet, L., Dommanget, F., Breton, V., & Evette, A. (2018). UsingSingle- and Multi-Date UAV and Satellite Imagery to Accurately Monitor Invasive Knotweed Species. Remote Sensing, 10(10), 1662.

22. Michez, A., Piégay, H., Jonathan, L., Claessens, H., & Lejeune, P. (2016). Mapping of riparian invasive species with supervised classification of Unmanned Aerial System (UAS) imagery. International Journal of Applied Earth Observation and Geoinformation, 44, 88-94.
23. Müllerová, J., Pyšek, P., Jarošík, V., & Pergl, J. (2005). Aerial Photographs as a Tool for Assessing the Regional Dynamics of the Invasive Plant Species Heracleum Mantegazzianum: Regional Dynamics of H. Mantegazzianum Invasion. Journal of Applied Ecology, 42(6), 1042-1053.
24. Naësset, E., & Økland, T. (2002). Estimating Tree Height and Tree Crown Properties Using Airborne Scanning Laser in a Boreal Nature Reserve. Remote Sensing of Environment, 79(1), 105-115.
25. Neupane, B., Horanont, T., & Aryal, J. (2021). Deep learning-based semantic segmentation of urban features in satellite images: A review and meta-analysis. Remote Sensing, 13(4), 808.
26. Nininahazwe, F., Théau, J., Marc Antoine, G., & Varin, M. (2023). Mapping Invasive Alien Plant Species with Very High Spatial Resolution and Multi-Date Satellite Imagery Using Object-Based and Machine Learning Techniques: A Comparative Study. GIScience & Remote Sensing, 60(1), 2190-203.
27. Niphadkar, M., & Nagendra, H. (2016). Remote Sensing of Invasive Plants: Incorporating Functional Traits into the Picture. International Journal of Remote Sensing, 37(13), 3074-3085.
28. Pyšek, P., & Prach, K. (1993). Plant Invasions and the Role of Riparian Habitats: A Comparison of Four Species Alien to Central Europe. Journal of Biogeography, 413-420.
29. Rijkswaterstaat. (2022, June 5). Dataregister Rijkswaterstaat.
30. Rouleau, G., Bouchard, M., Matte, R., & Lavoie, C. (2023). Effectiveness and cost of a rapid response campaign against Japanese knotweed (Reynoutria japonica) along a Canadian river. Invasive Plant Science and Management, 1-6.
31. Rouifed, S., Puijalon, S., Viricel, M. R., & Piola, F. (2011). Achene Buoyancy and Germinability of the Terrestrial Invasive Fallopia × Bohemica in Aquatic Environment: A New Vector of Dispersion? Ecoscience, 18(1), 79-84.

32. Royimani, L., Mutanga, O., Odindi, J., Dube, T., & Matongera, T. N. (2019). Advancements in Satellite Remote Sensing for Mapping and Monitoring of Alien Invasive Plant Species (AIPs). Physics and Chemistry of the Earth, Parts A/B/C, 112, 237-245.
33. Schenk, T., & Csathó, B. (2002). Fusion of LIDAR Data and Aerial Imagery for a More Complete Surface Description. International Archives of Photogrammetry Remote Sensing and Spatial Information Sciences, 34(3/A), 310-317.
34. Seiger, L. A., & Merchant, H. C. (1997). Mechanical Control of Japanese Knotweed (Fallopia Japonica [Houtt.] Ronse Decraene): Effects of Cutting Regime on Rhizomatous Reserves. Natural Areas Journal, 17(4), 341-345.
35. Shaw, R. H., & Seiger, L. A. (2002). Japanese Knotweed. Japanese Knotweed, 159-166.
36. Smith, J. M. D., Ward, J. P., Child, L. E., & Owen, M. R. (2007). A Simulation Model of Rhizome Networks for Fallopia Japonica (Japanese Knotweed) in the United Kingdom.
37. Štajerová, K., Šmilauer, P., Brůna, J., & Pyšek, P. (2017). Distribution of invasive plants in urban environment is strongly spatially structured. Landscape Ecology, 32, 681-692.
38. Gislason, P. O., Benediktsson, J. A., & Sveinsson, J. R. (2004, September). Random forest classification of multisource remote sensing and geographic data. In IGARSS 2004. 2004 IEEE International Geoscience and Remote Sensing Symposium (Vol. 2, pp. 1049-1052). IEEE.
39. van Iersel, W., Straatsma, M., Addink, E., & Middelkoop, H. (2018). Monitoring Height and Greenness of Non-Woody Floodplain Vegetation with UAV Time Series. ISPRS Journal of Photogrammetry and Remote Sensing, 141, 112-123.
40. Yue, S., Li, P., & Hao, P. (2003). SVM classification: Its contents and challenges. Applied Mathematics-A Journal of Chinese Universities, 18, 332-342.
41. Watson, G., & Watson, G. (2001). Knotweed and Bamboo in the United States: The problem and challenges. Weed Science, 49(6), 623-626.

42. Wu, M., Yang, L., Yu, B., Wang, Y., Zhao, X., Niu, Z., & Wang, C. (2014). Mapping crops acreages based on remote sensing and sampling investigation by multivariate probability proportional to size. Transactions of the Chinese Society of Agricultural Engineering, 30(2), 146-152.

43. Oplossing nabij: bladvlo lijkt effectief in bestrijding Japanse duizendknoop (nos.nl)

8 APPENDIX

(1) PleiadesNEO urban area 2023.06.04

(2) Superview - NEO riparian area 2023.05.27

(3) Superview – NEO riparian area 2023.03.02

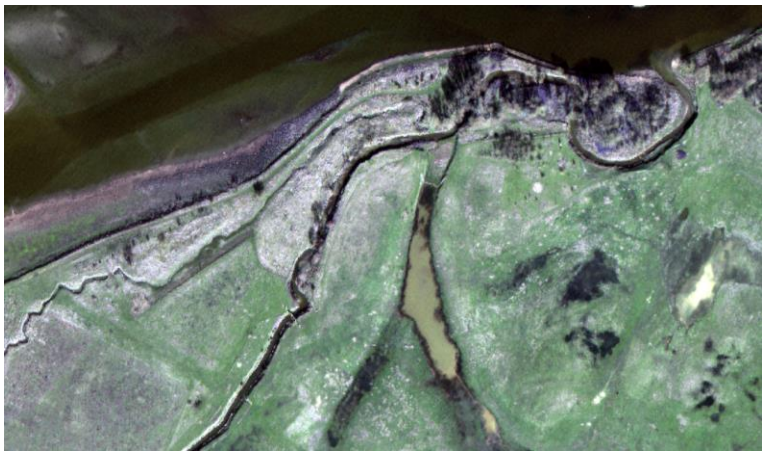

(4) Airborne image riparian area 2022

(5) Airborne image urban area 2022

(6) Segmented image of 2023.05.27

(7) Airborne images of mowed knotweed assignment in riparian area

Classes include respectively mowed Japanese knotweed, Water, Trees, Darker ground, Grass.

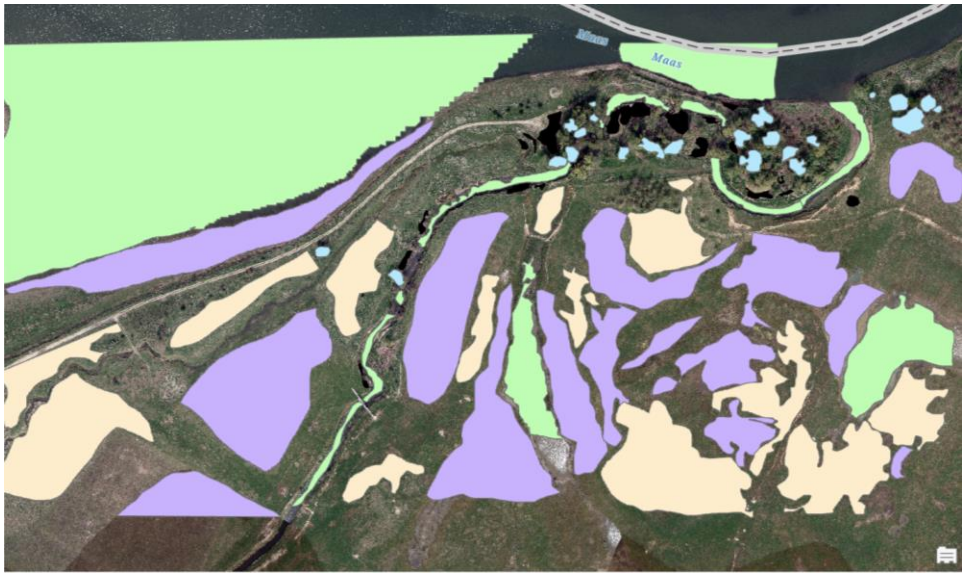

(8) Airborne images of mowed knotweed assignment in urban area.

Classes include respectively mowed Japanese knotweed, Non-Japanese knotweed vegetation, Impervious surfaces, Bare ground, Water.

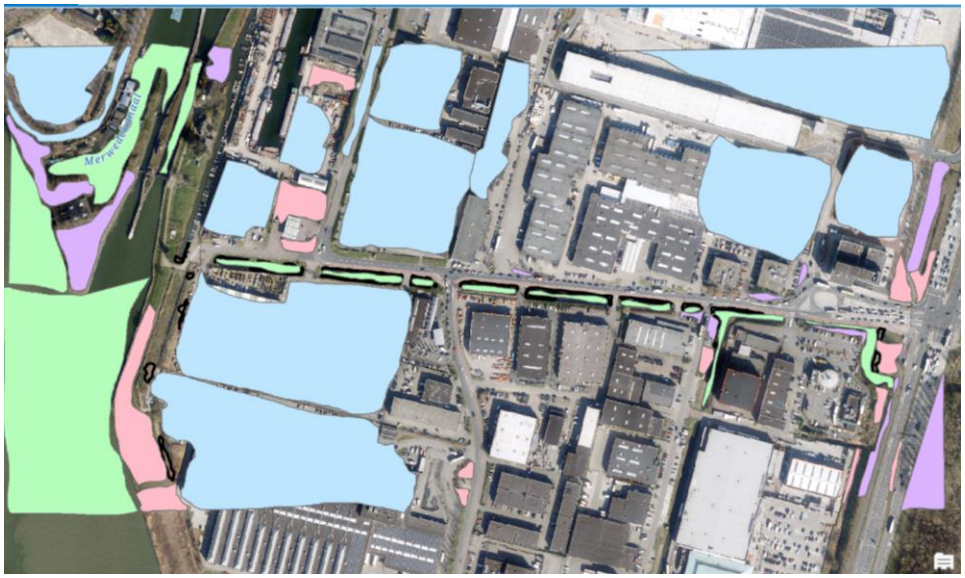

(9) Japanese knotweed visible in the images for urban and riparian area.

(10)Point cloud LiDAR 2022

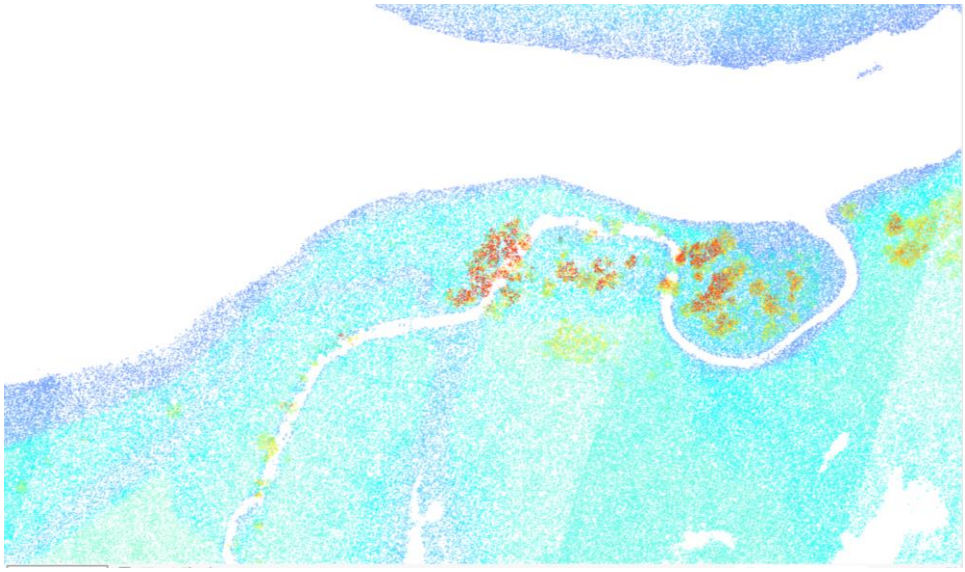

(11)Canopy Height Model (CHM)

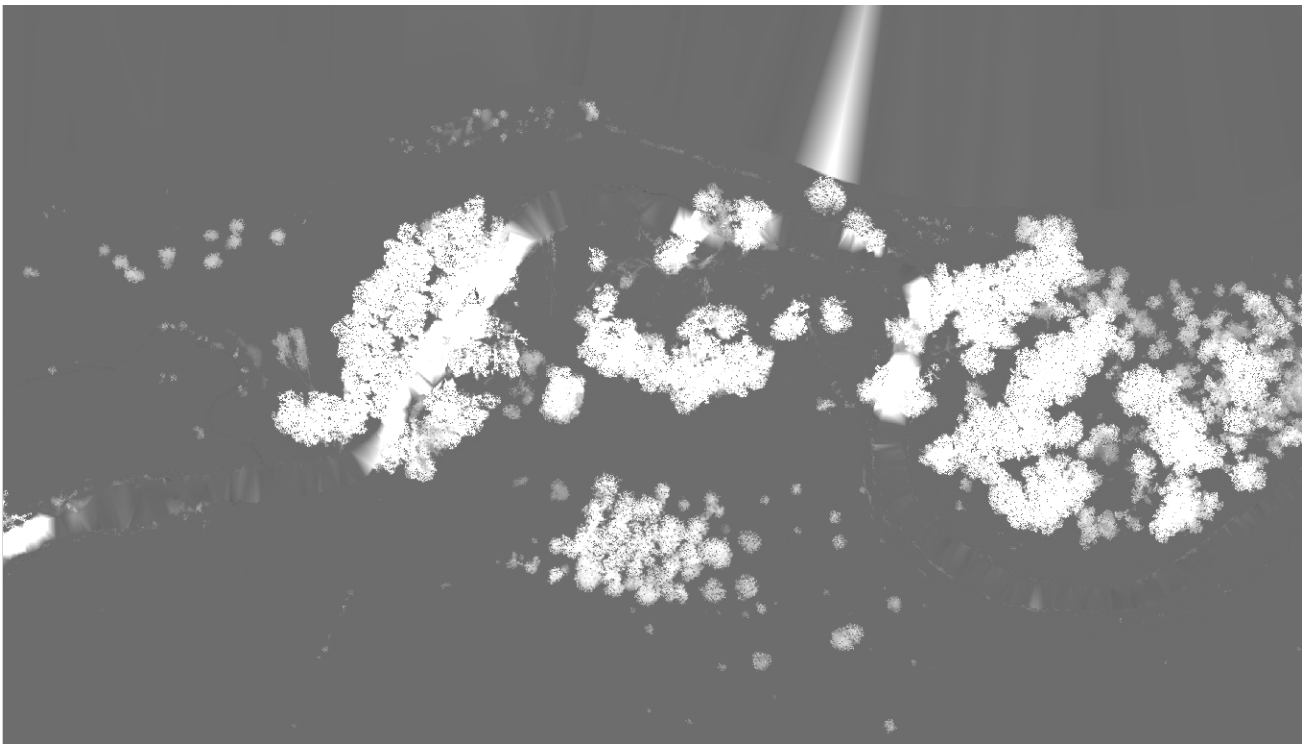

(12)Satellite imagery Light blue classes indicate Japanese knotweed assignment

Classes include respectively Japanese knotweed, Water, Other vegetation, Grass, Shrubs, Sand, Trees.

(13) Satellite imagery black classes indicate Japanese knotweed assignment

Classes include respectively Japanese knotweed, Water, Trees, Shrubs, Grass, Buildings, Cars, Roads.

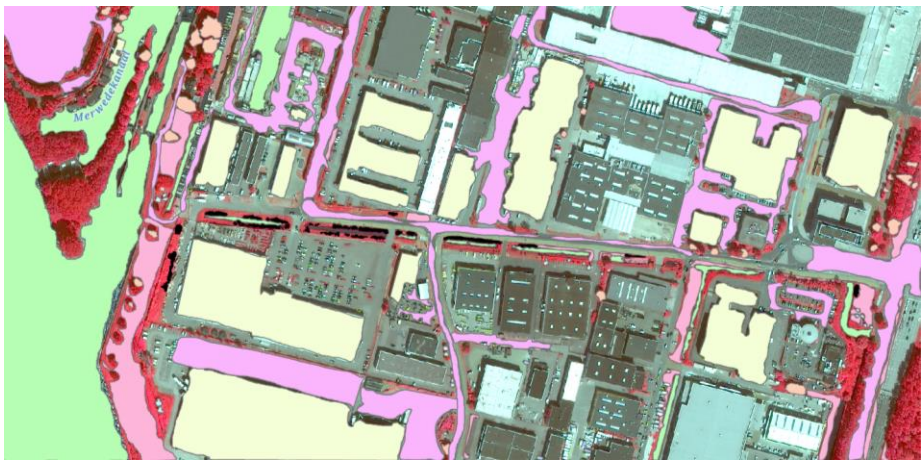

(14)NDVI values representation of urban area

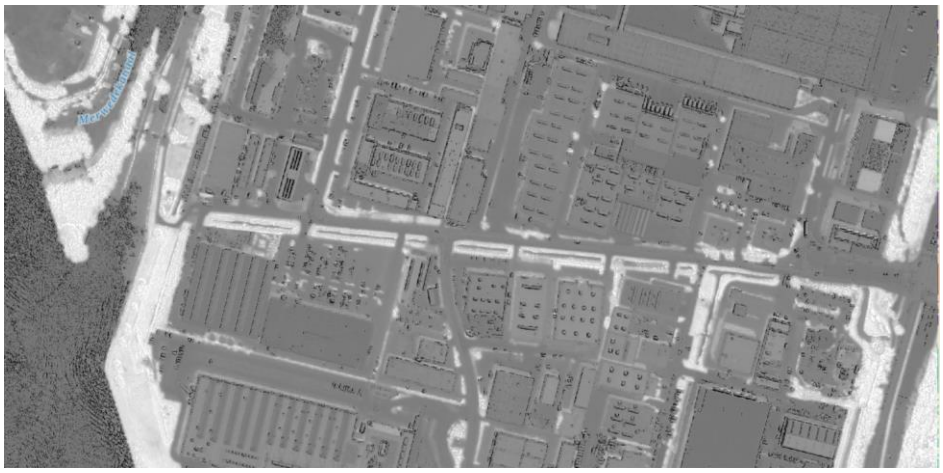

(15)NDVI values representation of riparian area

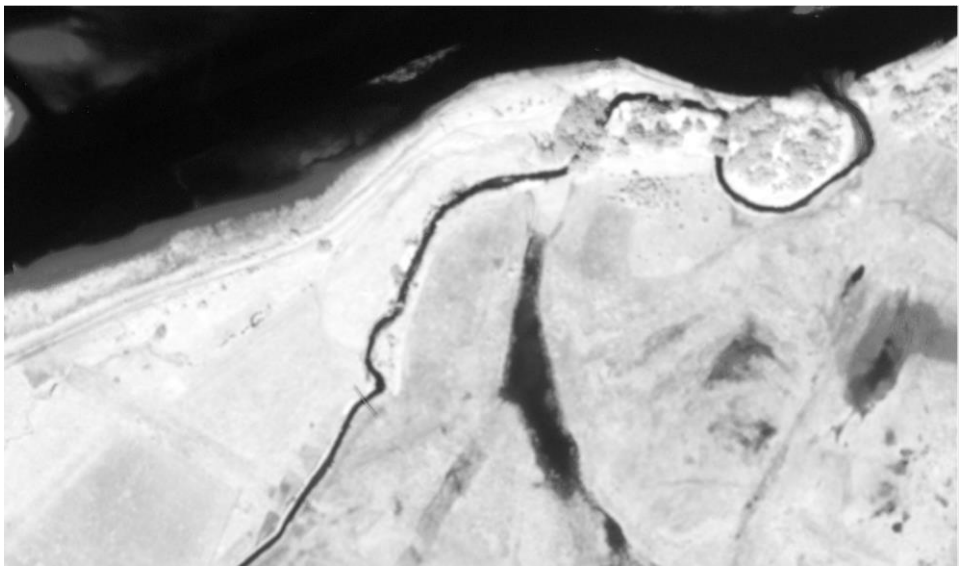

(16)NDVI values from ground truth data day 2023/05/27

Classes include respectively Japanese knotweed, water, other vegetation, grass, shrubs, sand and trees.

	OBJECTID *	Classvalue	FREQUENCY	MEAN_Value	MIN_Value	MAX_Value	MEDIAN_Value	STD_Value
1	1	1	440	1333.543182	1064	1554	1334.5	128.800204
2	2	2	892	986.438341	253	1454	990.5	266.120159
3	3	3	509	1233.239686	928	1488	1234	148.440056
4	4	4	392	1312.387755	1105	1508	1312.5	113.498888
5	5	5	272	1367.981618	1216	1505	1368.5	79.577086
6	6	6	653	1086.174579	677	1422	1087	190.848172
7	7	7	460	1289.843478	1019	1520	1290.5	134.064959

Click to add new row.

(17) Values from mowed period 2023/03/02

	OBJECTID *	Classvalue	FREQUENCY	MEAN_Value	MIN_Value	MAX_Value	STD_Value	MEDIAN_Value
1	1	1	550	879.381818	592	1187	161.03781	878.5
2	2	2	625	789.4352	446	1165	182.055639	789
3	3	3	612	921.655229	391	1230	179.659909	922.5
4	4	4	593	952.991568	10	1258	192.443274	961
5	5	5	549	949.413479	649	1269	161.253524	949
6	6	6	736	838.222826	8	1311	280.981418	867.5
7	7	7	610	919.085246	589	1227	178.311298	918.5
	Click to add new row.							

(18)Values from 2023/05/15 comparing a yearly difference

	OBJECTID *	Classvalue	FREQUENCY	MEAN_Value	MIN_Value	MAX_Value	MEDIAN_Value	STD_Value
1	1	1	465	1319.827957	1032	1568	1322	138.294758
2	2	2	738	1087.371274	715	1495	1087.5	214.071382
3	3	3	368	1312.630435	1127	1514	1312.5	106.68842
4	4	4	284	1337.658451	1196	1506	1337.5	82.417447
5	5	5	218	1383.43578	1268	1551	1382.5	65.848577
6	6	6	508	1161.661417	874	1446	1161.5	149.845731
7	7	7	411	1342.839416	1126	1613	1342	121.090224
	Click to add new row.							

(19)Pixel-based approach with SVM

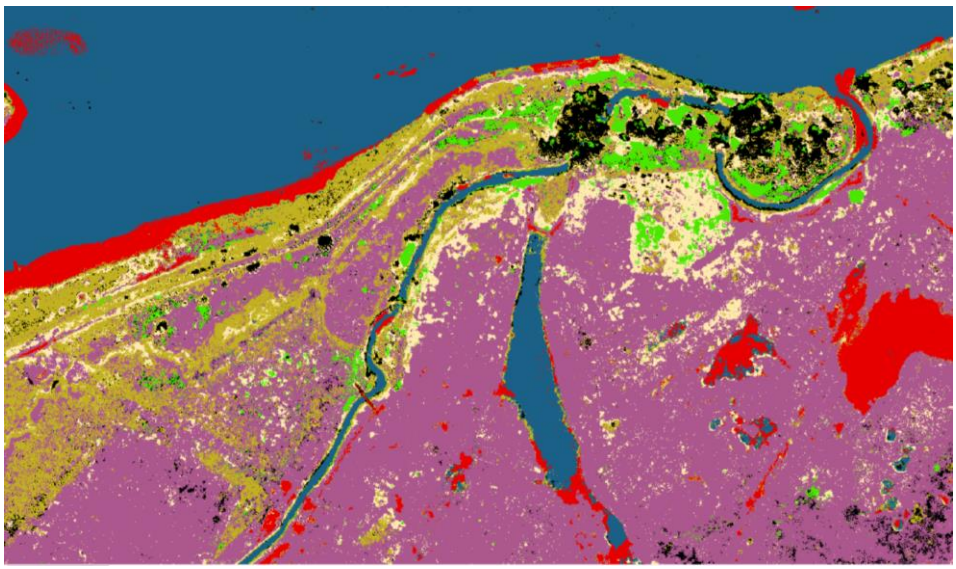

(20) Canopy Height Model with SVM

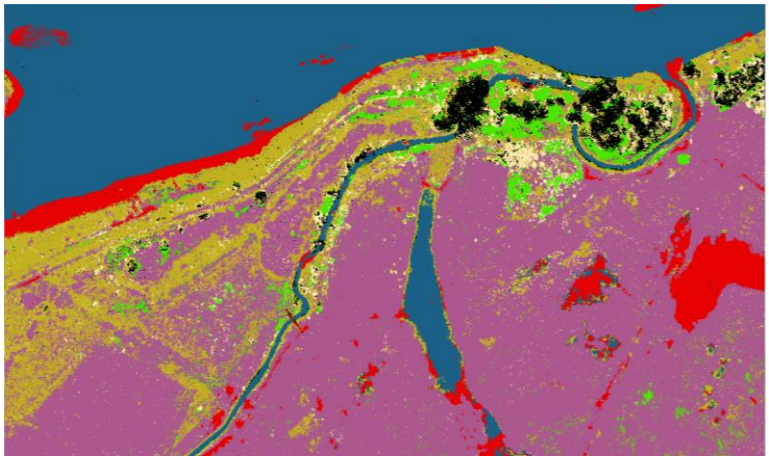

(21)NDVI with Pixel-based image analysis and SVM

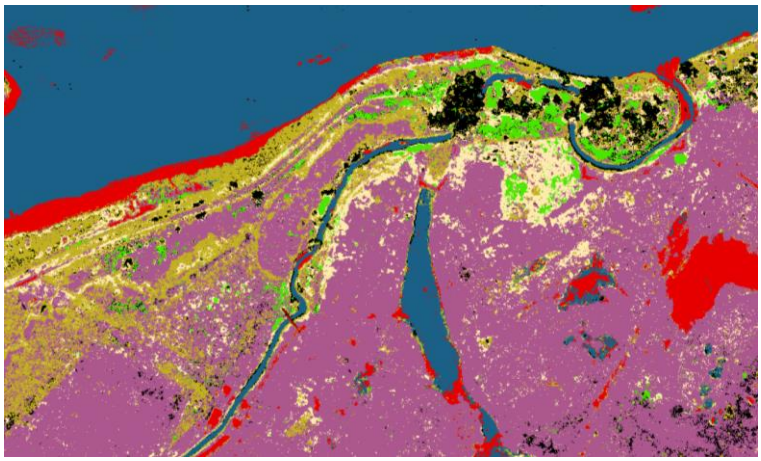

(22) Object-based image analysis with SVM

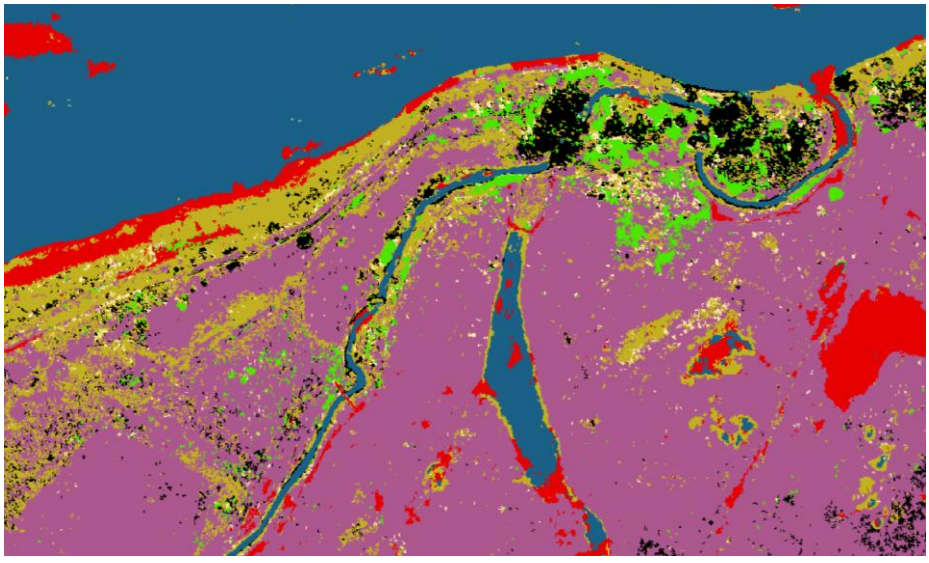

(23) Object-based image analysis with SVM in urban area

(24)Temporal analysis(TA)

2019.7.23

2019.09.20

2020.03.28

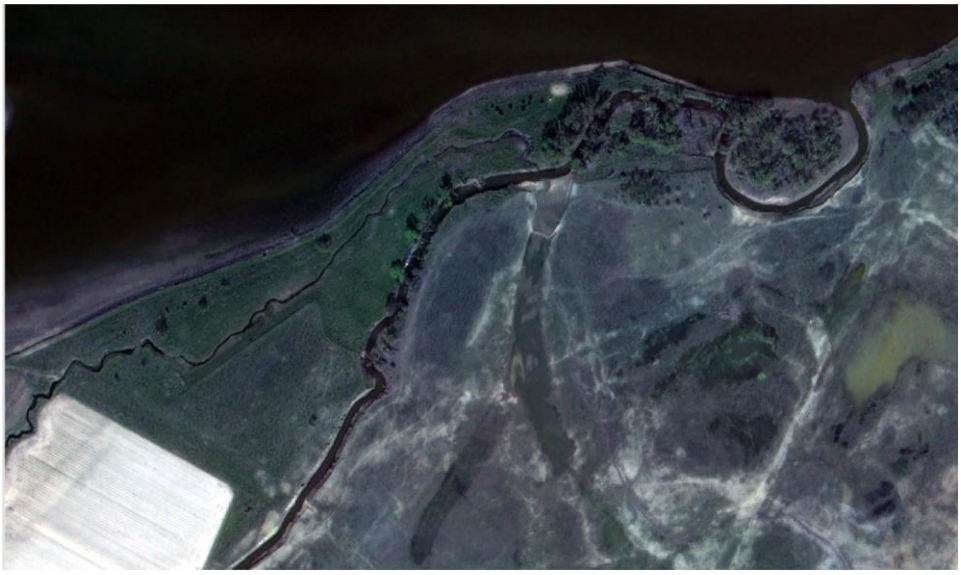

2020.6.23

2020.9.24

2020.11.24

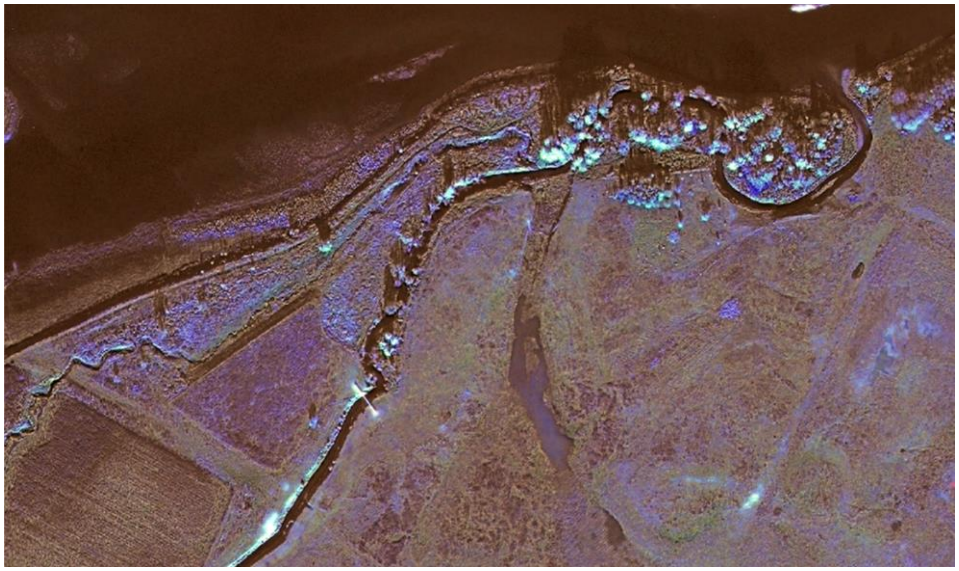

2021.03.20

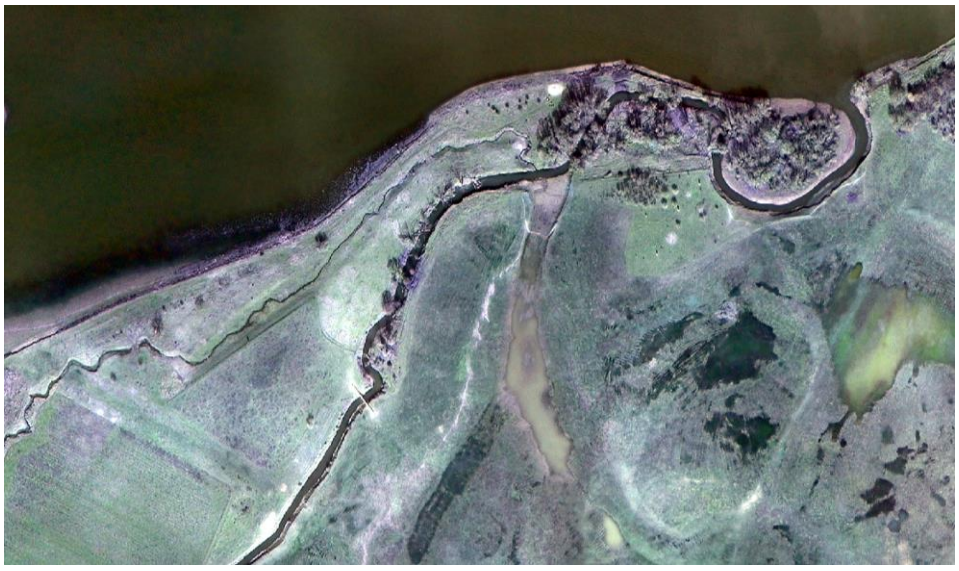

2021.06.08

2021.09.05

2021.12.16

2022.03.04

(25) 2022.05.15

2022.08.13

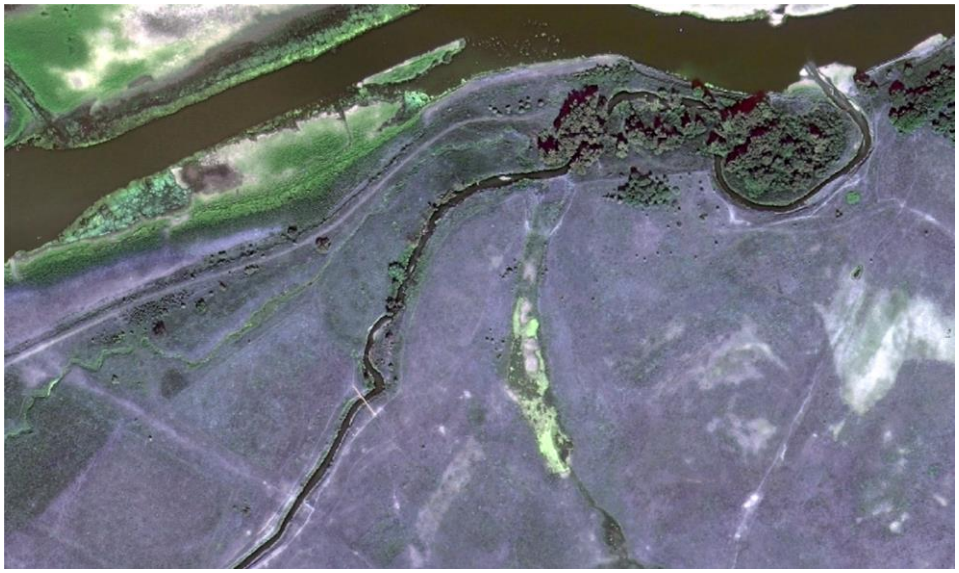

2022.11.01

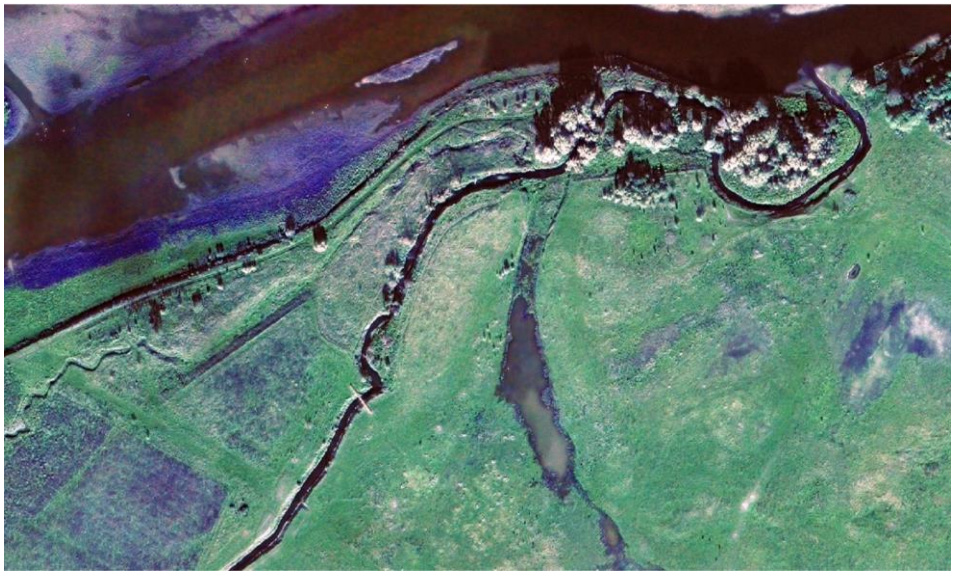

(26) Object-based image analysis with RT